

Available online at www.sciencedirect.com

ScienceDirect

www.elsevier.com/locate/matchar

Changes of shape memory properties in CuAlNi single crystals subjected to isothermal treatments



R. Gastien^{a,*}, C.E. Corbellani^a, V.E.A. Araujo^a, E. Zelaya^{b,c}, J.I. Beiroa^a,
M. Sade^{b,c,d}, F.C. Lovey^{b,d}

^aCentro de Investigaciones en Sólidos, CINSO-UNIDEF (MINDEF-CONICET), CITEDEF, J. B. de La Salle 4397, 1603 Villa Martelli, Buenos Aires, Argentina

^bDivisión Física de Metales, Centro Atómico Bariloche-CNEA, S.C. Bariloche, Argentina

^cConsejo Nacional de Investigaciones Científicas y Técnicas, Argentina

^dInstituto Balseiro, Universidad Nacional de Cuyo, Argentina

ARTICLE DATA

Article history:

Received 14 June 2013

Received in revised form

16 August 2013

Accepted 19 August 2013

Keywords:

Shape memory alloys

Martensitic transformations

Precipitation

Ordering processes

ABSTRACT

CuAlNi shape memory alloys are candidates for high temperature applications, mainly for their low diffusion at temperatures higher than room temperature. Aging thermal treatments made to the β -CuAlNi single crystal phase at 423 K were conducted in order to study how the main properties of these alloys change. Aging of the metastable β -phase above room temperature but well below the eutectoid point can favor a further ordering process started during quenching and trigger the decomposition of part of the alloy into more stable phases. Changes on the thermally and stress induced martensitic transformations were observed after these aging treatments, modifying the thermal and mechanical response of the material. Modifications of the metastable phase transformation diagrams are considered as well as the pseudoelastic fatigue behavior of the alloys.

© 2013 Elsevier Inc. All rights reserved.

1. Introduction

It is known that Cu based shape memory alloys are a cheaper alternative when compared with NiTi alloys for using them as actuator or sensor devices. Great efforts have been done to improve their mechanical response. Among Cu based alloys, Cu–Al–Ni alloys are an alternative for high temperature applications, such as sensors and/or actuators requiring their use above room temperature. There is a wide variety of applications, e.g. aerospace, automobile, petroleum and defense that require high temperature environment. The thermomechanical response plays a key role in actuator design. It is important then to know how the exposure of the alloy to these temperatures affects their thermal and mechanical properties, and finally how it affects their shape

memory and pseudoelastic properties [1–3]. For alloys with chemical composition around Cu–14Al–4Ni (wt.%) (Cu–28.13Al–3.70Ni in at.%), the high temperature body centered cubic phase can be obtained in a metastable state at room temperature after some quenching treatment [4]. During this process, the structure acquires a certain degree of order, and the final room-temperature phase is $L2_1$ type ordered one [5–7]. We will use the name β for the metastable $L2_1$ structure obtained after quenching and this phase is the parent structure which martensitically transforms in this material. There are two ways of inducing martensitic transformations from this β phase, one is by cooling below some critical temperature (we will call them TIM transformations: Thermally Induced Martensitic transformations) and the other way is by applying stress (called SIM transformations: Stress Induced Martensitic transformations)

* Corresponding author. Tel./fax: +54 11 4709 8228.

E-mail address: rgastien@citedef.gob.ar (R. Gastien).

[4,8–10]. The type of induced martensite depends on many factors, such as chemical composition of the alloy [11] (for TIM and SIM transformations) and crystal orientation, type of applied stress and test temperature [12–14] for SIM transformations. These martensitic transformations are the origin of the shape memory and pseudoelastic effects.

The thermodynamic behavior of CuAlNi single crystals, concerning martensitic phase transitions is well described by metastable phase diagrams [10]. Particularly, for compositions close to Cu–14.3Al–4.1Ni (wt.%), γ' martensite is obtained by temperature decrease and a well defined $\beta \rightarrow \beta'$ stress induced transition is obtained at temperatures at least 30 K above M_s , which is the main origin of the pseudoelastic behavior in these alloys. The stacking of two basal planes in the conventional cell characterizes the γ' while 18 basal planes form the conventional cell of the β' (18R) martensite. We are not considering here additional martensitic structures like α' (6R) which is obtained by tensile stressing β' at a well defined range of axis orientations [15].

The isothermal aging of the metastable β phase above room temperature but well below the eutectoid point of the alloy can trigger some ordering processes (assuming that the ordering was not completed during the quenching of the high-temperature β) as well as precipitation of the stable phases α (fcc) and/or γ (bcc) [16]. The final state of the alloy depends on its particular chemical composition and the isothermal treatment temperature and period [17–19] and it can affect the characteristic features of the TIM and SIM transformations [20–22].

The comprehension of the physical mechanisms which take place at temperatures above room temperature and their consequences on the thermomechanical properties are required for any possible use of the material. The present work focuses on the analysis of the effect of thermal aging at 423 K on the metastable phase diagram of CuAlNi single crystals. The selected composition, Cu–14.3Al–4.1Ni (wt.%), shows $\beta \rightarrow \gamma'$ transition by decreasing temperature. Mechanical behavior is analyzed by tensile tests, particularly focusing on the stress induced $\beta \rightarrow \beta'$ transition, including the pseudoelastic evolution if cycling is considered at test temperatures above room temperature.

The aim of this paper is to register the behavior of the TIM and SIM transformations that could be involved in pseudoelastic or shape memory applications of this alloy at temperatures higher than room temperature. For shape memory applications, it is important to know the changes in $\beta \leftrightarrow \gamma'$ TIM transformation upon thermal treatments. For applications that require the material going through a pseudoelastic cycle, it is important to improve the knowledge of the pseudoelastic transformation $\beta \leftrightarrow \beta'$ since the formation of stress induced γ' shows a wider hysteresis which might lead to the absence of retransformation during unloading. Due to this reason the authors focused the research on SIM $\beta \leftrightarrow \beta'$ transformations.

2. Experimental Procedure

Cu–14.3Al–4.1Ni (wt.%) alloys were obtained in a two step procedure: a) binary Cu–Ni alloys were prepared in an arc furnace and controlled Ar atmosphere and b) Al added in an

electric resistance furnace. In this way 20 g ternary alloys were used to grow single crystals at a well controlled speed in a temperature gradient (see [23] for details). Table 1 shows a list of the samples extracted from these crystals with their crystallographic orientation.

Aging thermal treatments at 423 K during different time intervals were performed to samples (20 × 3 × 1 mm) obtained from the single crystals and electrical resistance measurements were used to determine the characteristic temperatures M_s , M_f , A_s and A_f [24–26].

Specimens of cylindrical and plate-like shape for mechanical tests were prepared either mechanically or by spark erosion (gage length 20 mm). These samples had a subsequent heat treatment which consisted in an annealing at 1173 K for 1 h and quenching in a mix of water and ice, to eliminate any possible effects caused by locally heating of the sample during mechanization. After this heat treatment, their surfaces were mechanically and electrolytically polished. Tensile tests were carried out in a MTS Sintech 2/DL Machine, with a MTS 651 Environmental Chamber, and in an Instron 5567 machine with an Instron 3119-005 temperature chamber. The measurement of elongation was determined by the crosshead displacement. Tensile pseudoelastic cycles were performed at a crosshead speed equal to 0.2 mm/min and the pseudoelastic cycling at 5 mm/min ($1.7 \cdot 10^{-4} \text{ s}^{-1}$ and $4.2 \cdot 10^{-3} \text{ s}^{-1}$ respectively). The microstructure was observed by transmission electron microscopy using a FEI CM200 operated at 200 kV.

3. Results and Discussion

The effect of thermal treatments at 423 K on TIM transformations was studied measuring the electrical resistance of the sample in a cooling–heating cycle (heating and cooling rates are nearly equal, approx. 4 K/min). We analyzed changes in the critical temperatures (M_s , M_f , A_s and A_f), in the hysteresis width ($A_f - M_s$) and in the type of induced martensite.

In Fig. 1, a plot of $\Delta M_s = M_s(t) - M_s(0)$ vs. time of aging is shown. $M_s(0)$ represents the critical temperature M_s obtained after quenching, i.e. with no aging treatment, and $M_s(t)$ are the values of M_s obtained after aging the sample a time t at 423 K. It can be noted that ΔM_s increases with time and after 100 h of thermal treatment ΔM_s reaches an asymptotic value of approx. 23 K without changes in the hysteresis width. Non-crystal orientation dependence is observed in these results.

Table 1–Samples used in this paper with their crystallographic orientation. Nomenclature: A, B or C indicates the crystal the sample was extracted from.

Sample	Crystallographic orientation
A1	[105]
A2	[105]
A3	[105]
B1	[325]
B2	[325]
B3	[325]
C1	[001]
C2	[001]

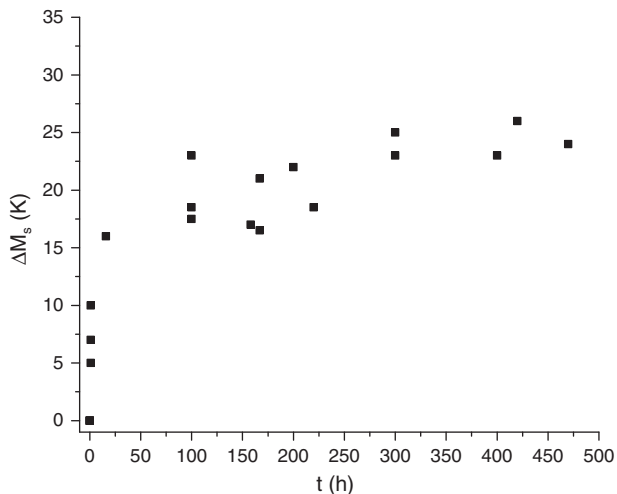


Fig. 1 – $\Delta M_s = M_s(t) - M_s(0)$ vs. t (aging time at 423 K). Error in ΔM_s is 1 K. Measurements from samples A1, A3, B1 and B2 were used for this graph.

The increase in M_s temperature can be understood taking into account that two processes can occur in the sample during aging. Some authors argued that for thermal treatments shorter than 100 h at 423 K, an ordering process is taking place during aging, assuming that some kind of disordering is present after quenching [27,28]. The second process that could happen is the precipitation of γ phase [21,22]. In a previous paper, the authors detected the presence of small precipitates in the β matrix in a sample aged 100 h at 423 K [23].

These precipitates are consistent with the low temperature stable γ phase as references [21,22] suggest. The structure of this phase is a complex bcc formed by $3 \times 3 \times 3$ bcc unit cells differing from β phase mainly in the Al content (by excess in the γ phase) and the interplanar distance by about 1%. This produces regions in the β matrix around the γ precipitates with lower aluminum content [29] which could increase the transformation temperatures [11].

A TEM dark field image of a sample subjected to 400 h at 423 K is shown in Fig. 2a. The image of those precipitates was obtained in a two beam condition using 114_γ , 115_γ , and $\bar{1}13_\beta$ spots. A double Moire contrast could be appreciated inside the precipitates due to the interference between β and γ structure. A zoom of the area inside a white rectangle is shown in the right upper side of the image in order to better appreciate the Moire effect. Fig. 2b shows a typical $[110]_\beta$ zone axis diffraction pattern of this sample where first and second order spots could be distinguished and very low intensity gamma spots could be appreciated forcing the contrast of the micrograph. This behavior could be attributed to the low size of the γ precipitates and also to the very low density of them in the entire sample.

The distribution of the observed precipitates was clearly inhomogeneous and particularly those precipitates shown in Fig. 2a were observed in the neighborhood of a dislocation. An average density of γ precipitation was determined for samples aged 400 h at 423 K and a value equal to 0.2 vol.% was obtained. The decrease of Al content of the β matrix can be

calculated from the quantity of γ phase present in the sample. An estimation of the M_s variation caused by this change of chemical composition of the β matrix can be done [11]. For this low concentration of γ precipitates, the estimated M_s variation is around 2 K, considering the composition of the γ precipitates as the corresponding one to the equilibrium γ phase. This fact implies that this low density of precipitation cannot be the main responsible of the M_s variation measured for a sample aged 400 h at 423 K that, as can be seen in Fig. 1, is around 25 K. For thermal treatments made at 423 K, small γ precipitates can be seen at least after 100 h of aging [23] but their low density and size cannot justify the changes observed in the induced martensitic transformations. This statement considers that precipitates can induce variation in M_s through composition changes in the β matrix.

Nakamura et al. [30] studied the aging effects in Cu–Al–Ni alloys with different concentrations of Ni. They argued that ordering of β and the precipitation of γ phase during quenching and on subsequent aging, are retarded by the addition of Ni because the diffusion of Al and Cu is suppressed. They determined that for alloys with concentration of Ni higher than 3 at.%, the ordering of the DO_3 structure is not completed during quenching but continues in the subsequent type of ordered structure, accompanied by a rise in M_s temperature. They also noted that this ordering was observed prior to the precipitation of γ phase.

Other authors [31] noted that the formation of γ phase and highly ordered domains decreases the matrix solute content and consequently increases the M_s temperature in Cu–14Al–4Ni (wt.%) thin foils. Van Humbeeck et al. [32] showed that ordering in β phase is a multiple activated process, influencing simultaneously the physical and mechanical properties of the martensite. The behavior of these properties is moreover influenced by defect annihilation and defect rearrangements.

Taking into account this bibliographic review and the fact that a small density of γ precipitates was observed in Cu–14.3Al–4.1Ni (wt.%) alloy aged at 423 K, the increase observed in M_s temperature is likely to be originated in ordering processes without a noticeable influence of γ precipitates.

On the other hand, the effect of thermal treatments on stress induced martensitic transformations was studied by tensile mechanical tests made before and after thermal aging treatments. Tests were focused on the $\beta \leftrightarrow \beta'$ SIM transformation, as was explained in the Introduction.

Tensile pseudoelastic cycles were performed at different temperatures. Critical stresses for transformation and retransformation were determined for each test temperature at 2% of transformation strain. The hysteresis width was inferred as the difference between both critical stresses. To study the evolution of critical stresses and hysteresis width with aging time, pseudoelastic cycles were performed at a constant test temperature, after different periods of aging for each sample. Average values of the critical stresses obtained for each aging time were plotted vs. time. An example of this procedure made on sample B3 is shown in Fig. 3. It was found that both critical stresses decrease with aging time at 423 K, but the decrease in the retransformation stress is more pronounced. Similar results were obtained with sample C1. This fact implies that the hysteresis width of the pseudoelastic cycles increases slightly with time. The increase of the hysteresis width of the SIM

transformations after aging is probably due to the interaction between precipitates and the martensitic transformation. No effect of further ordering on hysteresis is expected since the

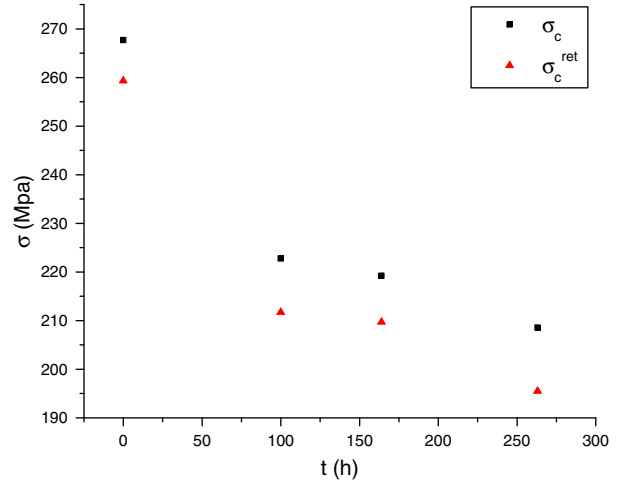
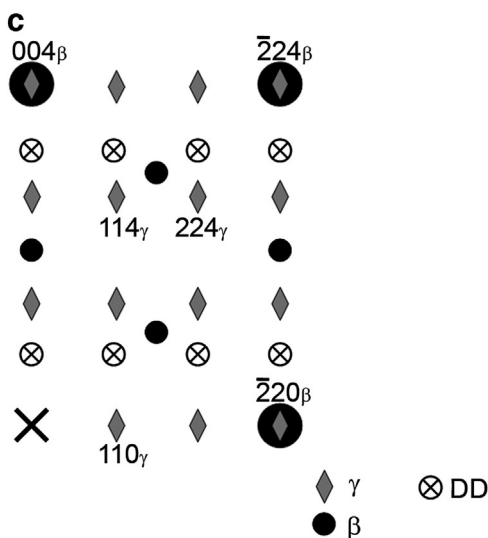
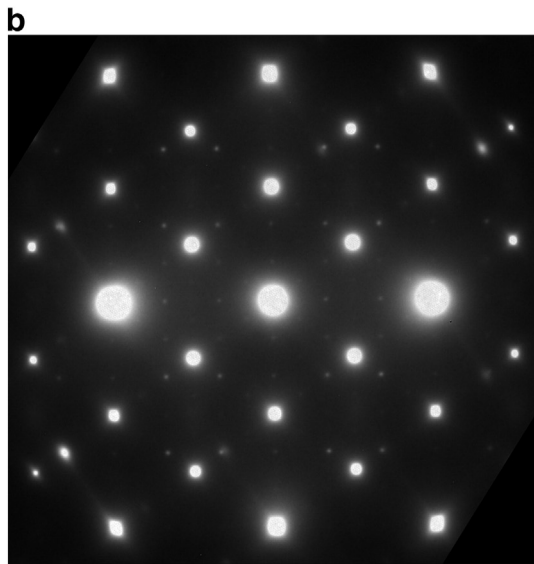
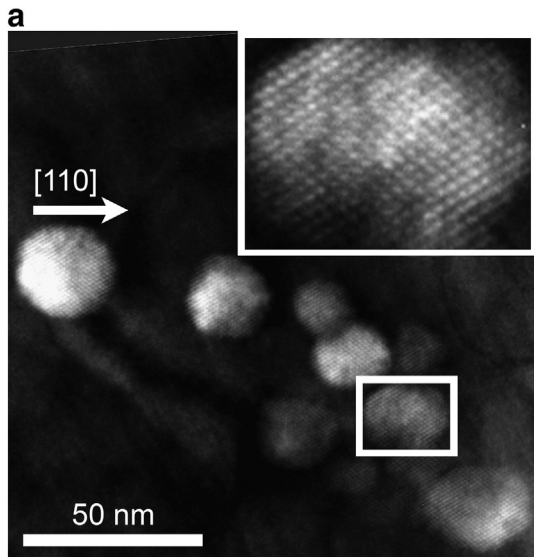


Fig. 3 – Critical stresses for transformation (σ_c) and retransformation (σ_c^{ret}) vs. aging time at 423 K for sample B3. Errors in σ_c and σ_c^{ret} are approx 0.2%.

main effect of changing the order of the parent structure is a shift of the Gibbs free energy of this phase with no change in the driving forces of the direct and reverse transformations.

Other authors have studied the interaction of single variant martensitic transformation with small γ precipitates in Cu–Zn–Al shape memory alloys [33,34]. In these alloys, the presence of small precipitates (around 7 nm) causes an increment of the hysteresis width. They argued that the interaction of the martensite with the precipitates is mainly related to the shape of the matrix cavity containing them upon transformation. The driving force or excess of free energy associated to the hysteresis is quantitatively related to the creation of dislocations and subsequent deformation process of the martensite around the precipitates.

The critical stress for SIM transformations (for the forward transformation) decreases as t at 423 K increases, as observed in Fig. 3. A more comprehensive picture of this behavior is obtained if the σ –T phase transformation diagram is obtained. This has been performed for samples thermally treated at different time intervals at 423 K and results are shown in Fig. 4, where critical applied stresses are plotted vs. test temperature for each different thermal treatment. Results for the as quenched sample are also included. From this figure it is clear that a linear Clausius–Clapeyron relationship is well defined for the as-quenched sample and after 115 h at 423 K. No noticeable change is detected in the slopes of the linear relationships obtained indicating that the same entropy change between β and β' is obtained in the selected temperature range for the

Fig. 2 – a) TEM dark field image of sample B3 subjected to 400 h at 423 K. A zoom of the area inside the white rectangle is shown in the upper side of the image. b) A typical diffraction pattern of a $[100]_\beta$ zone axis with precipitates. Low intensity gamma spots could be distinguished. c) Key diagram of the top right hand part of the diffraction pattern shown in (b). Diamond symbols stand for γ phase while the round symbols stand for β phase.

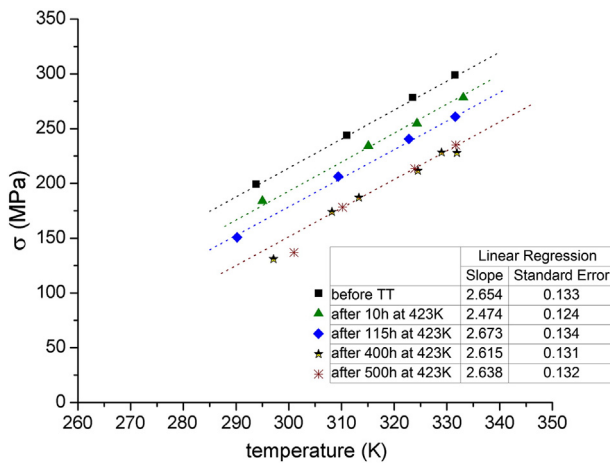


Fig. 4 – σ - T diagrams for sample C2 after different thermal treatments at 423 K. Error in σ is approx 0.2%. Linear regression results corresponding to each thermal treatment are included. Slopes and their Standard Error are in (MPa/K).

mentioned thermal treatments. A small deviation is observed at low temperatures for isothermal aging during intervals equal to 400 and 500 h respectively. This deviation comes from the fact that those points correspond to $\beta \rightarrow \beta' + \gamma'$ and a deviation from linearity arrives when γ' martensite nucleates [35]. The other noticeable point is that the linear curves describing the Clausius–Clapeyron relationship shift as aging time at 423 K increases except at the highest time intervals where an overlapping is observed (see points obtained after 400 and 500 h in Fig. 4).

For the purpose of comparing the effects of thermal aging on SIM and TIM transformations, the shift in the σ - T diagrams can also be meant as a temperature shift (called ΔT_{SIM}), which can be obtained at constant stress. As was explained previously, the σ - T lines made at different periods of aging were parallel and move to the right as time of aging increases. The fact that the lines were nearly parallel each other indicates that the entropy associated to the $\beta \rightarrow \beta'$ transformation is not altered by aging, so the shift of these lines can be associated to a M_s temperature shift (the temperature at which these lines intersect the temperature axis corresponds to zero applied stress and means that the transformation is thermally induced, so this temperature is equal to M_s). In this way, the shift of these lines can be understood as a temperature shift. A plot of ΔT_{SIM} vs. aging time at 423 K is presented in Fig. 5. This behavior can be compared with the plot of ΔM_s vs aging time at 423 K from Fig. 1. It can be noted that in both cases (SIM and TIM transformations) the temperature shift (ΔM_s and ΔT for TIM and SIM transformations respectively) has the same behavior: an important increase around 100 h of thermal treatment and an asymptotic behavior after 400 h of aging. It is noticeable that the shift of ΔM_s and ΔT_{SIM} for TIM and SIM transformations respectively is nearly of the same value. This fact supports that ordering processes are also the main responsible for the observed changes in the critical stress to transform.

Recarte et al. [36] determine shifts in temperatures of transformation after thermal aging at 473 K, and consider that

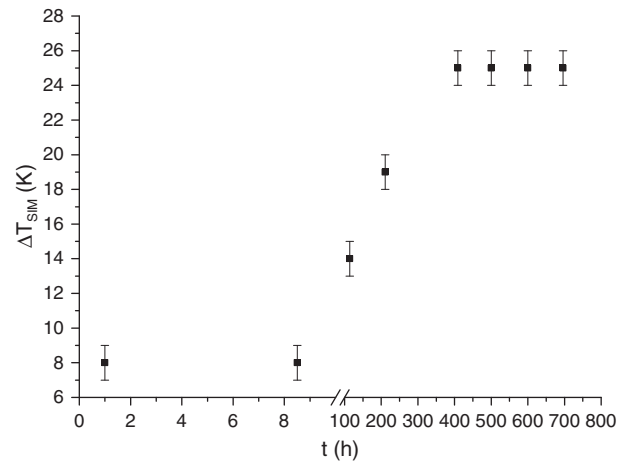


Fig. 5 – ΔT_{SIM} (K) vs. t (time aging at 423 K). ΔT_{SIM} represents the temperature shift of the σ - T diagrams for C2 sample. Errors bars are shown.

changes in order are also the main reasons to explain the observed measurements. In that paper the authors have also found that $\beta \rightarrow \beta'$ transformation evolves into $\beta \rightarrow \beta' + \gamma'$ martensitic transition. In the present manuscript the analysis of the pseudoelastic transitions at different temperatures allows one to precisely separate the formation of both martensites as it has been shown in Fig. 4.

Pseudoelastic cycling, i.e. repeated cycles through the $\beta \rightarrow \beta'$ SIM transformation, was made at temperatures above room temperature after different time intervals at 423 K. Significant change neither in the critical stress nor in the hysteresis width was observed during cycling after thermal treatments. In Fig. 6a, values of σ_c (critical stress for $\beta \rightarrow \beta'$ transformation) and σ_c^{ret} (critical stress for $\beta' \rightarrow \beta$ retransformation) are plotted vs. number of pseudoelastic cycles (N). In Table 2, different tests were arranged in increasing order of the time elapsed in the aging treatment, indicating the number of $\beta \rightarrow \beta'$ cycles made on the samples. Averages of variation of critical stress for $\beta \rightarrow \beta'$ transformation and $\beta' \rightarrow \beta$ retransformation are shown in the same table.

An example of the σ - ϵ (stress–strain) curves during cycling is shown in Fig. 6b. The fact that critical stresses and hysteresis width of the cycles remained unchanged after aging is an important fact to take into account for applications, particularly in the case of devices that will be used as an actuator, which will be forced to do the transformation–retransformation cycle many times during its lifetime. The stability of the mechanical behavior for larger number of cycles for a sample with 700 h at 423 K is shown in Fig. 6c.

Finally it is interesting to notice that at the present temperature of aging an asymptotic behavior is reached considering either thermally induced or stress induced transformations. In both cases the main measurable effect is either an increase of martensitic transformation temperatures or a decrease in the corresponding critical stresses to transform. However the main shape memory properties are not affected. The present results indicate that at large time intervals at 423 K, an asymptotic state of order is reached

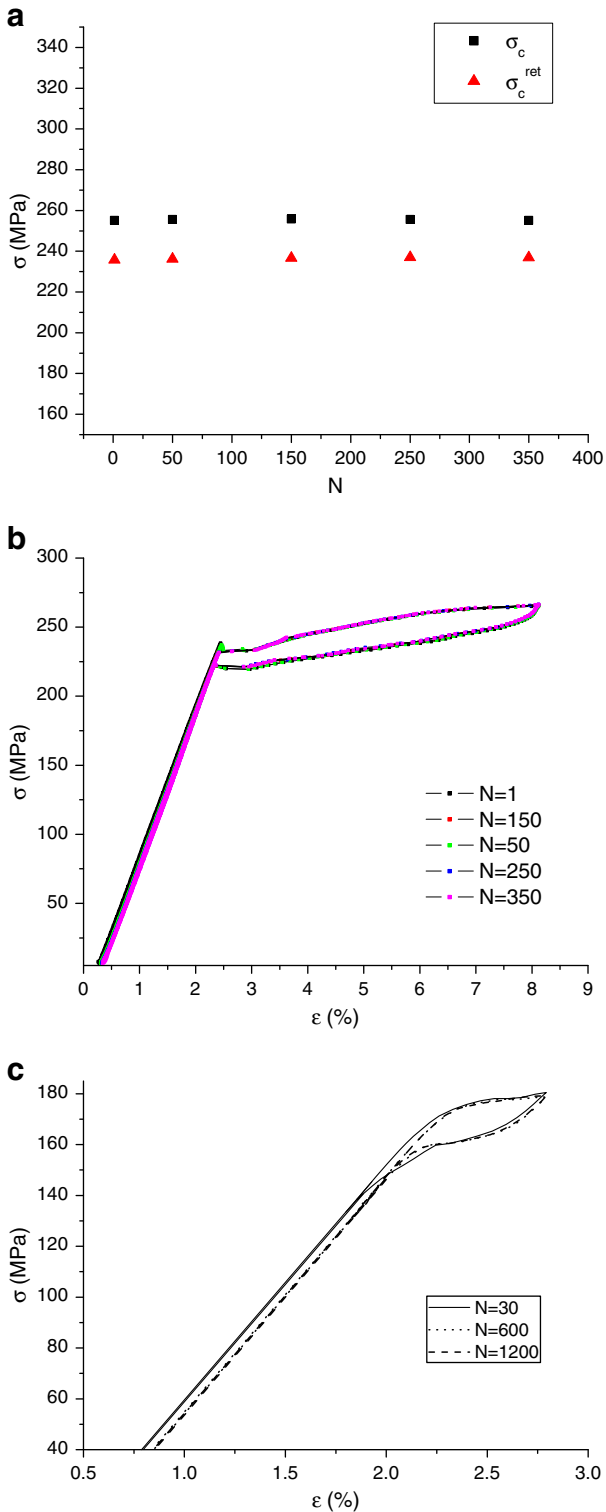


Fig. 6 – a) Critical stresses for transformation (σ_c) and retransformation (σ_c^{ret}) vs. N (number of cycles) for $\beta \leftrightarrow \beta'$ cycling made on A2 sample at 333 K after aging 15 h at 423 K. Error in σ is approx 0.3%. b) σ (stress) vs. ϵ (strain) curves for the same sample as a), cycles $N = 1, 50, 150, 250$ and 350 are shown, error in σ is approx 0.3%. c) σ (stress) vs. ϵ (strain) curves of a $\beta \leftrightarrow \beta'$ cycling made on C2 sample at 323 K after 700 h at 423 K. $N = 30, 600$ and 1200 cycles are shown. Error in σ is approx 0.3%.

Table 2 – Average variation (%) of σ_c and σ_c^{ret} during cycling, for different aging treatments at 423 K.

Aging time at 423 K (h)	Number of cycles (N) $\beta \leftrightarrow \beta'$	Test temperature (K)	Average variation of σ_c during cycling (%)	Average variation of σ_c^{ret} during cycling (%)
0	1000	323	-0.47	-0.29
15	350	333	0.16	0.39
115	540	303	-2.88	3.29
125	110	296	0.44	0.74
265	900	325	-1.71	-0.66
700	1400	323	-1.92	-0.35

leading to a stable behavior concerning martensitic transformations, while the kinetics related to precipitation of stable phases remains negligible. The latest point can be rationalized by a high driving force overwhelmed by a rather weak diffusion at temperatures equal or lower than 423 K.

4. Conclusions

Changes on SIM and TIM transformations were observed after thermal treatments made at 423 K on Cu-14.3Al-4.1Ni (wt.%) single crystals. These changes are most probably due to ordering processes than precipitation. Precipitation of γ phase exists in a very low density, leading to a negligible influence on martensitic transformation temperatures and a weak influence on the mechanical hysteresis of the $\beta \rightarrow \beta'$ transition.

The variation of critical stress and transformation temperatures after aging is controllable as they show an asymptotic behavior after approx 100 h of thermal treatment.

Moreover, pseudoelastic cycling made at temperatures above room temperature on samples aged at 423 K shows repeatable mechanical response up to 1000 cycles.

These features are promising for thinking this alloy for applications that require their use after being aged at temperatures equal to or lower than 423 K.

Acknowledgments

The authors thank C. Gómez and T. Carrasco for their help in single crystal growth, F. de Castro Bubani and P. Riquelme for their technical support in mechanical tests, and P.B. Bozzano and G. Zbihlel for the assistance in sample preparation and TEM observation of the samples.

The financial support from SSICyDT-Ministerio de Defensa (PIDDEF 015/11), Agencia Nacional de Promoción Científica y Tecnológica (PICT 2284-07) and Universidad Nacional de Cuyo (Proyecto 06/C387) is gratefully acknowledged.

REFERENCES

[1] Kannarpady GK, Bhattacharyya A, Pulnev S, Vahhi IJ. The effect of isothermal mechanical cycling on Cu-13.3Al-4.0Ni (wt.%) shape memory alloy single crystal wires. *J Alloys Compd* 2006;425:112–22.

- [2] Kannarpady GK, Trigwell S, Bhattacharyya A, Pulnev S, Viahhi I. Effect of an overheating temperature on cyclic isothermal stress-induced transformations in single crystal Cu–13.3Al–4.0Ni (wt.%) shape memory alloys. *Mech Mater* 2006;38:493–509.
- [3] Song G, Ma N. Robust control of a shape memory alloy wire actuated flap. *Smart Mater Struct* 2007;16:51–7.
- [4] Otsuka K, Sakamoto H, Shimizu K. Successive stress-induced martensitic transformations and associated transformation pseudoelasticity in Cu–Al–Ni. *Acta Metall* 1979;27:585–601.
- [5] Recarte V, Lambri OA, Pérez-Sáez RB, Nó ML, San Juan J. Ordering temperatures in Cu–Al–Ni shape memory alloys. *J Appl Phys Lett* 1997;70:3513–5.
- [6] Pérez-Landazábal JI, Recarte V, Pérez-Sáez RB, Nó ML, Campo J, San Juan J. Determination of the next-nearest neighbor order in β phase in Cu–Al–Ni shape memory alloys. *Appl Phys Lett* 2002;81:1794–6.
- [7] Nakata Y, Tadaki T, Shimizu K. Site determination of Ni atoms in Cu–Al–Ni shape memory alloys by electron channelling enhanced microanalysis. *Mater Trans (JIM)* 1990;31:652–8.
- [8] Gastien R, Corbellani CE, Álvarez Villar HN, Sade M, Lovey FC. Pseudoelastic cycling in Cu–14.3Al–4.1Ni (wt.%) single crystals. *Mater Sci Eng A* 2003;349:191–6.
- [9] Gastien R, Corbellani CE, Sade M, Lovey FC. Thermal and pseudoelastic cycling in Cu–14.3Al–4.1Ni (wt.%) single crystals. *Acta Mater* 2005;53:1685–91.
- [10] Gastien R, Corbellani CE, Sade M, Lovey FC. A σ –T diagram analysis regarding the γ' inhibition in $\beta \leftrightarrow \beta' + \gamma'$ cycling in CuAlNi single crystals. *Scr Mater* 2006;54:1451–5.
- [11] Recarte V, Pérez-Sáez RB, Bocanegra EH, Nó ML, San Juan J. Dependence of the martensitic transformation characteristics on concentration in Cu–Al–Ni shape memory alloys. *Mater Sci Eng A* 1999;273–275:380–4.
- [12] Novák V, Malimánek J, Zárubová N. Martensitic transformation in [110] single crystals of Cu–Al–Ni alloy. *Key Eng Mater* 1994;97–98:419.
- [13] Novák V, Malimánek J, Zárubová N. Martensitic transformations in single crystals of Cu–Al–Ni induced by tensile stress. *Mater Sci Eng A* 1995;191:193–201.
- [14] Novák V, Sittner P, Vokoun D, Zárubová N. On the anisotropy of martensitic transformations in Cu–base alloys. *Mater Sci Eng A* 1999;273–275:280–4.
- [15] de Castro Bubani F, Sade M, Lovey FC. Improvements in the mechanical properties of the 18R \leftrightarrow 6R high-hysteresis martensitic transformation by nanoprecipitates in CuZnAl alloys. *Mater Sci Eng A* 2012;543:88–95.
- [16] Dunne DP, Kennon NF. Ageing of copper-based shape memory alloys. *Met Forum* 1981;4:176–83.
- [17] Tadaki T. Cu-based shape memory alloys. In: Otsuka K, Wayman CM, editors. *Shape memory materials*. Cambridge: Cambridge U. Press; 1998. p. 97–116.
- [18] Rodriguez P, Guenin G. Thermal aging behaviour and origin of a CuAlNi shape memory alloy. *Mater Sci Eng A* 1990;129:273.
- [19] Kennon NF, Dunne DP, Middleton L. Aging effects in copper-based shape memory alloys. *Trans A* 1982;13:551–5.
- [20] Van Humbeeck J, Van Hulle D, Delaey L, Ortín J, Seguí C, Torra V. A two-stage martensite transformation in a Cu–13.99 mass% Al–3.5 mass% Ni alloy. *Trans Jpn Inst Met* 1987;28:383–91.
- [21] Picornell C, Pons J, Cesari E. Effects of thermal ageing in beta-phase in Cu–Al–Ni single crystals. *J Phys IV France* 1997;7C5:323–8.
- [22] Zarubova N, Gemperle A, Novak V. Ageing phenomena in a Cu–Al–Ni alloy. *J Phys IV France* 1997;7C5:281–6.
- [23] Gastien R, Corbellani CE, Bozzano PB, Sade M, Lovey FC. Low temperature isothermal ageing in shape memory CuAlNi single crystals. *J Alloys Compd* 2010;495:428–31.
- [24] Zengin R, Ceylan M. Influence of neutron irradiation on the characteristics of Cu–13%wt.Al–4%wt.Ni shape memory alloys. *Mater Lett* 2004;58:55–9.
- [25] Pelosin V, Gerland M, Rivière A. First stage of the structural evolution of austenite in Cu–Al–Ni shape memory alloys. *EPJ Appl Phys* 2001;15:15–21.
- [26] Recarte V, Lambri OA, Pérez-Sáez RB, Nó ML, San Juan J. Ordering temperatures in Cu–Al–Ni shape memory alloys. *Appl Phys Lett* 1997;70:3513–5.
- [27] Cingolani E, Van Humbeeck J, Ahlers M. Stabilization and two-way shape memory effect in Cu–Al–Ni single crystals. *Metal Mater Trans A* 1999;30:493–9.
- [28] Recarte V, Pérez-Sáez RB, Nó ML, San Juan J. Ordering kinetics in Cu–Al–Ni shape memory alloys. *J Appl Phys* 1999;86:5467–73.
- [29] Doherty RB. Diffusive phase transformations in the solid state. In: Cahn RW, Haasen P, editors. *Physical metallurgy*. 4th ed. North-Holland; 1996. p. 1363–506.
- [30] Nakamura F, Kusui J, Shimizu Y, Takamura J. Martensitic transformation and the aging effect in Cu–Al–Ni alloys. *J Jpn Inst Met* 1980;44:1302–11.
- [31] Kuwano N, Wayman CM. Some effects of parent phase aging on the martensitic transformation in a Cu–Al–Ni shape memory alloy. *Metal Trans A* 1984;15:621–6.
- [32] Van Humbeeck J, Chandrasekaran M, Delaey L. The influence of post quench ageing in the beta-phase on the transformation characteristics and the physical and mechanical properties of martensite in a Cu–Al–Ni shape memory alloys. *ISIJ Int* 1989;29:388–94.
- [33] Roqueta DO, Lovey FC, Sade M. Martensite–austenite stability shifts due to the presence of gamma-phase precipitates in Cu–Zn–Al alloys. *Scr Mater* 1999;10:1359–13565.
- [34] Lovey FC, Torra V, Isalgué A, Roqueta D, Sade M. Interaction of single variant martensitic transformation with small gamma type precipitates in Cu–Zn–Al. *Acta Metall Mater* 1994;42:453–60.
- [35] Gastien R, Corbellani CE, Sade M, Lovey FC. Thermodynamical aspects of martensitic transformations in CuAlNi single crystals. *Scr Mater* 2004;50:1103–7.
- [36] Recarte V, Pérez-Sáez RB, Nó ML, San Juan J. Evolution of martensitic transformation in Cu–Al–Ni shape memory alloys during low-temperature aging. *J Mater Res* 1999;14:2806–13.